PROCEEDINGS OF SCIENCE

Resolved Millisecond Pulsars are Consistent with the Galactic Center Excess.

Harrison Ploeg and Chris Gordon*

School of Physical and Chemical Sciences, University of Canterbury, Christchurch, New Zealand

Roland Crocker

Research School of Astronomy and Astrophysics, Australian National University, Canberra, Australia

Oscar Macias

Center for Neutrino Physics, Department of Physics, Virginia Tech, Blacksburg, VA 24061, USA

Fermi Large Area Telescope data reveal an excess of GeV gamma rays from the direction of the Galactic Center and bulge. Several explanations have been proposed for this excess including an unresolved population of millisecond pulsars (MSPs) and self-annihilating dark matter. It has been claimed that a key discriminant for or against the MSP explanation can be extracted from the properties of the luminosity function describing this source population. Specifically, is the luminosity function of the putative MSPs in the Galactic Center consistent with that characterizing the resolved MSPs in the Galactic disk? To investigate this we have used a Bayesian Markov Chain Monte Carlo to evaluate the posterior distribution of the parameters of the MSP luminosity function describing both resolved MSPs and the Galactic Center excess. At variance with some other claims, our analysis reveals that, within current uncertainties, both data sets can be well fit with the same luminosity function.

5th Annual Conference on High Energy Astrophysics in Southern Africa
4-6 October, 2017
University of the Witwatersrand (Wits), South Africa

*Speaker.

PoS(HEASA2017)020

1. Introduction

This article is a summarised version of ref. [1]. An extended γ-ray source has been found [2, 3, 4, 5, 6, 7, 8, 9, 10, 11, 12, 13] in the *Fermi* Large Area Telescope (*Fermi*-LAT) data covering the central $\sim 10^\circ$ of the Milky Way. This Galactic Center Excess (GCE) signal has a spectral peak at about 2 GeV and reaches a maximum intensity at the Galactic Center (GC) from where it falls off radially like $\propto r^{-2.4}$. Given its morphological and spectral characteristics, the GCE might constitute the indirect signature of the self-annihilation of dark matter particles distributed in a Navarro-Frenk-White (NFW) like density profile.

However, recent statistical studies [14, 15, 16] may have uncovered, as dim clusters of photons, a population of unresolved, point-like sources in the GCE γ-ray signal. These studies thus suggest, contrary to the dark matter hypothesis, that the GCE is actually attributable to many dim, unresolved point sources, presumably of stellar origin (though note it has also been argued that the photon clusters are merely due to variations in the gamma-ray flux associated with the small scale structure of the diffuse Galactic emission [17]). A natural explanation of these γ-ray sources (were they real and of stellar origin) is that they are millisecond pulsars (MSPs) [18, 4, 6, 19] and/or young pulsars [20] which both have GeV-peaked gamma-ray spectra (also see [21]).

This prompts the immediate question: what is the origin of this putative MSP and/or pulsar population? The pulsar hypothesis requires relatively recent star formation given the $\lesssim$ few Myr γ-ray lifetimes of ordinary pulsars. Such star formation is absent from most of the bulge except in the $r \lesssim 100$ pc nuclear region; a young pulsar explanation of the GCE thus requires that the bulge be populated with pulsars that are launched out of the nucleus. It has been claimed that this can be achieved rather naturally by the pulsar's natal kicks [20]. On the other hand, MSPs can be generated (in a number of ways: see below) from old stellar populations. Rather generically, two broad classes of bulge stellar population might be at play here: the bulge field stars or the bulge stars that were born in high redshift globular clusters that have been accumulated into the inner Galaxy by dynamical friction and disrupted by tidal forces over the lifetime of the Milky Way [22]. Note that while the fraction of the bulge stellar population that derives from disrupted globular clusters is only at the $\sim$ few percent level [23], observationally, globular cluster environments are orders of magnitude more efficient per unit stellar mass at producing MSPs [24] than field stellar populations.

2. Methods

We used 71 MSPs found within the Fermi-LAT third source catalog (3FGL) [25]. In the 3FGL, MSPs are not distinguished from pulsars and so the Galactic disk MSPs were identified by searching the Australia Telescope National Facility (ATNF) pulsar catalog [26] for 3FGL pulsars with periods of less than 10 milliseconds and which were not associated with globular clusters. A small number of additional MSPs were identified through the use of an online list and found in the 3FGL catalog[1].

[1] https://confluence.slac.stanford.edu/display/GLAMCOG/Public+List+of+LAT-Detected+Gamma-Ray+Pulsars

2.1 Modeling a Population of Millisecond Pulsars

To simulate the GCE and a population of observed MSPs to compare with data, the underlying population of MSPs must be modeled. This requires spatial and luminosity models and, for the MSPs around the GC that may be responsible for the excess, a distribution of spectra.

As in ref. [27], we used a lognormal luminosity function. The lognormal distribution is one in which the logarithm of luminosity is normally distributed, its probability density function is:

$$p(L) = \frac{1}{\sigma_L L\sqrt{2\pi}} \exp\left(\frac{-(\ln(L) - \ln(L_{\text{med}}))^2}{2\sigma_L^2}\right) \tag{2.1}$$

where L is luminosity, L_{med} is the median luminosity, and $\ln(L_{\text{med}})$ and σ_L are the mean and standard deviation of the normal distribution in $\ln(L)$.

The spatial distribution of MSPs was divided into two components. One of these components models a population of MSPs scattered throughout the Milky Way disk according to the following density distribution [28]:

$$\rho_{\text{disk}}(r_{\text{cyl}}, z, N_{\text{disk}}) = \frac{N_{\text{disk}}}{4\pi\sigma_r^2 z_0} \exp\left(-r_{\text{cyl}}^2/2\sigma_r^2\right) \exp(-|z|/z_0) \tag{2.2}$$

where r_{cyl} is the distance from the GC projected onto the Galactic plane, z is the distance perpendicular to the Galactic plane, N_{disk} is the total number of MSPs in the entire Galactic disk, and σ_r and z_0 are scale parameters. We take the distance from us to the GC to be 8.25kpc.

The second component of the spatial distribution models the bulge population of MSPs potentially contributing to the GCE. In our region of interest, this density distribution has been found to be fitted by a spherically symmetric power law profile [2, 3, 4, 5, 6, 7, 8, 10, 11, 13]. In this article we use the parameterization

$$\rho_{\text{bulge}}(r, N_{\text{bulge}}) = \frac{3N_{\text{bulge}}}{20\pi r_{\text{bulge}}^{0.6}} r^{-2.4}, \quad 0 \le r < r_{\text{bulge}} \tag{2.3}$$

where N_{bulge} parameter is the total number of bulge MSPs in the Galaxy, r is the distance from the GC, and r_{bulge} is the maximum radial extent of the bulge. The power law index is only known to about 20% accuracy, but our results are insensitive to this variation. We used a bulge radius of $r_{\text{bulge}} = 3.1$ kpc to be consistent with ref. [27]. This is also the value determined from the COBE-DIRBE NIR maps [29].

Once the positions and luminosities of a population of MSPs (in both the disk and bulge) were simulated, an observed population could be found by applying a detection threshold based on the flux of each MSP, where the relationship between flux F, luminosity L and distance d is:

$$F = \frac{L}{4\pi d^2} \tag{2.4}$$

A resolved MSP is one for which $F \ge F_{\text{th}}$, where F_{th} is the threshold flux. The second Fermi-LAT catalog of gamma-ray pulsars [30] included an attempt to find the detection threshold as a function of l and b by adding simulated point sources at different positions in the sky and determining what the minimum flux needed was before they were detected. As the sensitivity to point sources

depends strongly on the gamma-ray background, the detection threshold is highest near the Galactic plane. As in ref. [27], our modeled threshold did not solely depend on location in Galactic coordinates. Instead, $F_{\rm th}$ was drawn from a lognormal distribution for each simulated MSP:

$$p(F_{\rm th}) = \frac{1}{\sigma_{\rm th} F_{\rm th}\sqrt{2\pi}} \exp\left[\frac{-(\ln(F_{\rm th}) - (\mu_{\rm th}(l,b) + K_{\rm th}))^2}{2\sigma_{\rm th}^2}\right] \tag{2.5}$$

where $K_{\rm th}$ and $\sigma_{\rm th}$ are parameters, and $\mu_{\rm th}(l,b)$ is the natural logarithm of the threshold flux at l and b according to the pulsar catalog. A map of $2\exp(\mu_{\rm th}(l,b))$ is given in figure 16 of ref. [30].

The authors of ref. [30] point out that these reported detection thresholds are likely to be underestimates; $K_{\rm th}$ is included as a parameter to account for this. The purpose of drawing $F_{\rm th}$ from the lognormal distribution is to approximate the variation that may occur due to uncertainty in the estimated threshold, or characteristics specific to individual pulsars, such as their spectra or light curves. The consequence of this is that the detection probability of a pulsar increases with flux, and does so particularly rapidly around the median of the threshold distribution, $\mu_{\rm th}(l,b) + K_{\rm th}$.

To simulate the GCE, a distribution of spectra must be modeled for the bulge MSPs. In the 3FGL catalog sources were fitted with three different spectral shapes. One of these is a power law:

$$\frac{{\rm d}N}{{\rm d}E} \propto \left(\frac{E}{E_0}\right)^{-\Gamma} \tag{2.6}$$

The second is an exponentially cutoff power law:

$$\frac{{\rm d}N}{{\rm d}E} \propto \left(\frac{E}{E_0}\right)^{-\Gamma} \exp\left(-\frac{E}{E_{\rm cut}}\right) \tag{2.7}$$

Finally, a log parabolic spectrum was fitted for a small number of the observed MSPs:

$$\frac{{\rm d}N}{{\rm d}E} \propto \left(\frac{E}{E_0}\right)^{-\omega-\beta\ln(E/E_0)} \tag{2.8}$$

Each simulated bulge MSP was assigned the spectral shape and best fit parameters of a random resolved MSP. The proportionality constant was then found by requiring the energy integral over the spectrum (from 0.1 to 100 GeV) be equal to the flux of the simulated MSP:

$$F = \int_{0.1\ {\rm GeV}}^{100\ {\rm GeV}} E\frac{dN}{dE}dE \tag{2.9}$$

The simulated gamma-ray excess was then the sum of the spectra of all the MSPs in the relevant region of interest. This region is the $7^\circ \times 7^\circ$ box around the Galactic Center in the case of the spherically symmetric bulge.

2.2 Markov Chain Monte Carlo

In Subsection 2.1 a model was described which can produce a simulated population of MSPs, decide which are resolved, and simulate a gamma-ray excess based on the bulge MSP population. To find the parameters which may best reproduce the data, it is necessary to have a method for

randomly sampling an arbitrary and potentially complex probability distribution of any number of dimensions. The adaptive Metropolis MCMC algorithm described in ref. [31] was used for this.

We used an unbinned Poisson distribution for the likelihood of the resolved MSPs [32]:

$$\mathscr{L}_{\rm res} \propto \exp(-\lambda_{\rm res}) \prod_{i=1}^{N} \rho(l_i, b_i, d_i, F_i) \tag{2.10}$$

where $N = 71$ is the number of resolved MSPs, $\lambda_{\rm res}$ is the expected number of resolved MSPs, $\rho(l_i, b_i, d_i, F_i)$ is the modeled density of resolved MSPs at Galactic coordinates l_i, b_i, distance d_i, and flux F_i.

We used the following parameters (θ):

1. The total expected number of observed MSPs $\lambda_{\rm res}$ from eq. (2.10).
2. The natural log of the ratio of total number of disk to bulge MSPs $\ln\left(r_{\rm d/b}\right) = \ln\left(N_{\rm disk}/N_{\rm bulge}\right)$ from eqs. (2.3) and (2.2).
3. Luminosity function parameters $\log_{10}(L_{\rm med})$ and σ_L for the lognormal distribution given by eq. (2.1).
4. The flux threshold distribution parameters $K_{\rm th}$ and $\sigma_{\rm th}$ from eq. (2.5).
5. The spatial model parameters σ_r and z_0.
6. The distance parameter for each observed MSP, d_i.
7. The parallax distance measurement probability parameter α.
8. The flux of each observed MSP, F_i.
9. The flux threshold at each observed MSP, $F_{{\rm th},i}$.

Note that $\lambda_{\rm res}$ appears as a parameter (rather than being fixed to the observed number of MSPs) because the observed number is essentially drawn from a Poisson distribution with an unknown expected value. The parameters $\lambda_{\rm res}$ and $\sigma_{\rm th}$ were required to be greater than 0 and σ_L was restricted to values above 0.5. A lower limit of 0.8 for σ_L is justified in ref. [27] by considering the luminosity distribution of those MSPs with parallax distance measurements. Here, those measurements were included as priors on the distance parameters corresponding to those MSPs. The upper limit for σ_r was 10.0, this was chosen as it is expected to be approximately 5 kpc [33, 28, 34, 35, 27]. Prior boundaries were also used for other parameters, these boundaries were located in places where the likelihood was very low (i.e. the proposed set of parameters would be extremely unlikely to be accepted).

We do not use the dispersion estimates of the MSPs distances as they may have a high systematic error [30, 27].

The expected excess that would be produced by the bulge MSPs can be found by multiplying $N_{\rm bulge}$ by the expected contribution of a single MSP. The large size of the resulting bin meant that it was necessary to take $\left(\frac{{\rm d}N}{{\rm d}E}\right)_{{\rm sim},i}$ to be the mean across the bin, $N/(E_{{\rm max},i} - E_{{\rm min},i})$, where $E_{{\rm min},i}$ and

$E_{\mathrm{max},i}$ are the edges of the bin. So as the counts in each bin are reasonably high, the GCE likelihood will be well approximated [36] by a Gaussian:

$$\mathscr{L}_{\mathrm{GCE}} \propto \prod_{i=1}^{N} \exp\left(-\left(\left(\frac{\mathrm{d}N}{\mathrm{d}E}\right)_{\mathrm{sim},i} - \left(\frac{\mathrm{d}N}{\mathrm{d}E}\right)_{\mathrm{data},i} \right)^2 / (2\sigma^2_{\mathrm{data},i}) \right) \tag{2.11}$$

where $\left(\frac{\mathrm{d}N}{\mathrm{d}E}\right)_{\mathrm{sim},i}$ and $\left(\frac{\mathrm{d}N}{\mathrm{d}E}\right)_{\mathrm{data},i}$ are respectively the simulated and observed gamma-ray excess with uncertainty $\sigma^2_{\mathrm{data},i}$ at E_i. This is calculated using the GCE spectra from refs. [6] and [37].

The second component of the likelihood $\mathscr{L}_{\mathrm{res}}$ is given by eq. (2.10) with

$$\rho(l_i, b_i, d_i, F_i) \propto (\rho_{\mathrm{disk}} + \rho_{\mathrm{bulge}}) p(L_i) d_i^4 \tag{2.12}$$

where $p(L_i)$ is the luminosity function given by eq. (2.1), the factor d_i^4 is from a product of a factor of d_i^2 from the Jacobian for the change of variables F_i to L_i and another factor of d_i^2 from the Jacobian for the change of variables from Cartesian to Galactic coordinates as ρ_{disk} and ρ_{bulge} are densities in Cartesian coordinates. Also, ρ_{disk} and ρ_{bulge} are determined by eqs. (2.2) and (2.3) respectively. For our prior distribution we used:

$$p(\theta) \propto \prod_{i=1}^{N} p(F_{\mathrm{th},i}) p(F_i | F_{\mathrm{data},i}, \sigma_{\mathrm{data},i}) \prod_{i \in \mathrm{parallax}} p(d_i) \tag{2.13}$$

where $p(F_{\mathrm{th},i})$ is given by eq. (2.4), $p(F_i | F_{\mathrm{data},i}, \sigma_{\mathrm{data},i})$ is a normal distribution with the observed MSP's flux and uncertainty (obtained from 3FGL) as the mean and standard deviation respectively and $p(d_i)$ is constructed for the subset of MSPs which had parallax measurements using the best fit value and errors.

As parallax measurements are more likely to be available for nearer MSPs, a third component of the likelihood was used. This $\mathscr{L}_{\mathrm{parallax}}$ is the product of modeled probabilities of observed MSPs having or not having a parallax distance measurement:

$$\mathscr{L}_{\mathrm{parallax}} = \prod_{i \in \mathrm{parallax}} \exp(-d_i/\alpha) \prod_{i \notin \mathrm{parallax}} (1 - \exp(-d_i/\alpha)) \tag{2.14}$$

The posterior distribution was obtained by combining the likelihood and prior distributions:

$$p(\theta | \mathrm{data}) \propto \mathscr{L}_{\mathrm{res}} \times \mathscr{L}_{\mathrm{GCE}} \times \mathscr{L}_{\mathrm{parallax}} \times p(\theta) \tag{2.15}$$

We marginalized over the $F_{\mathrm{th},i}$ and the F_i variables using numerical integration. The other variables were sampled using the MCMC. Twelve Markov chains were constructed of five million iterations each for the spherical.

Although, we have a large number of parameters that we are fitting, this is ameliorated as the flux (F_i) and distance parameters (d_i) are all linked by the geometric model (eqs. (2.2) and (2.3) given by eq. (2.1). Also, the threshold parameters $(F_{\mathrm{th},i})$ are linked by the threshold prior giving by eq. (2.5). This regularizes the problem in a similar way to ridge regression [38].

3. Discussion

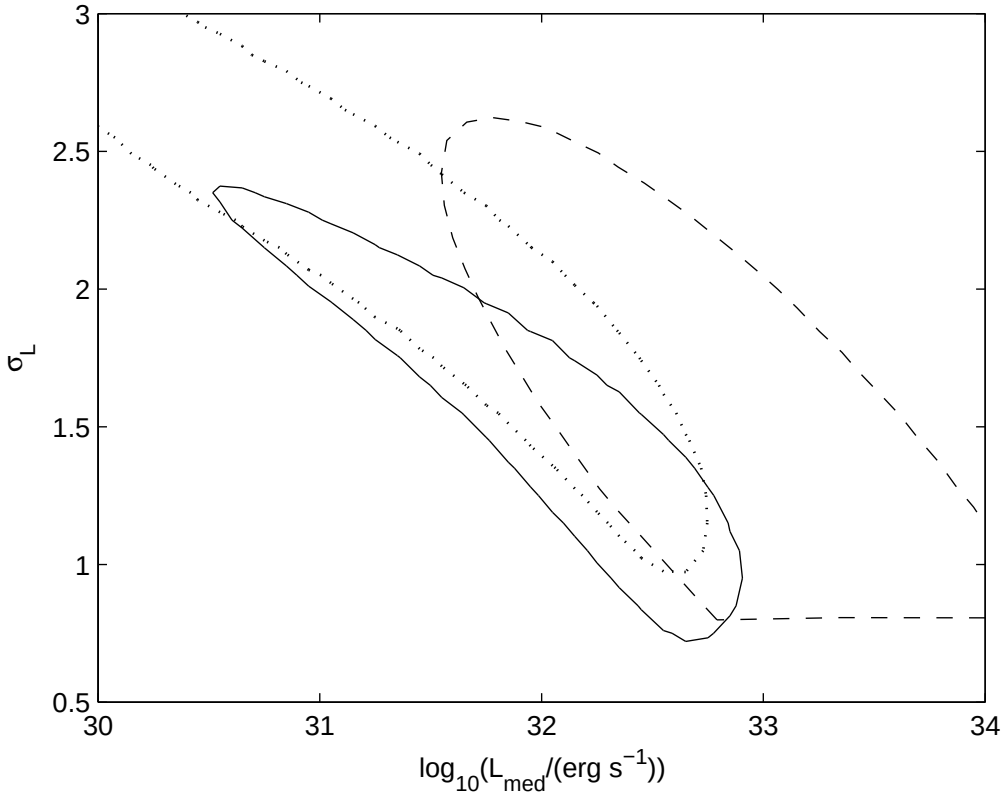

Figure 1: Contour plot of luminosity function parameter distribution showing the 95% contour for the log-normal luminosity distribution and spherical bulge model. The dashed line is the 2σ contour from ref. [27]. The dotted line is the 95% contour for the luminosity function distribution assuming the spherical bulge does not contribute to resolved MSPs.

Ref. [27] used the observed MSPs to attempt to find parameters for the lognormal luminosity function by using the product of three binned likelihoods one for longitude, one for latitude, and the other for flux [39]. In each bin the expected number of observations λ_i was found by taking a large number of random samples from the model, binning them, and normalizing so that $\sum_{i=1}^{N}\lambda_i = 66$, where 66 was the number of MSPs used in their fit. Their likelihood for each distribution was:

$$\mathscr{L} = \prod_i \frac{\lambda_i^{n_i}\exp(-\lambda_i)}{n_i!} \tag{3.1}$$

where n_i was the number of observed MSPs in bin i. The results are compared to the results of this work in figure 1. While there is some agreement, the difference could be explained in part by the use of the parallax measured distances which were only used to estimate a lower bound on σ_L in ref. [27]. The other significant difference between that study and this work is the separable form of likelihood they used. As seen from eq. (2.10), the actual likelihood will not be separable in this way. We included, in addition, the bulge model as part of the likelihood, not only to find parameters fitting the GCE, but also because some luminosity distributions could result in many observed

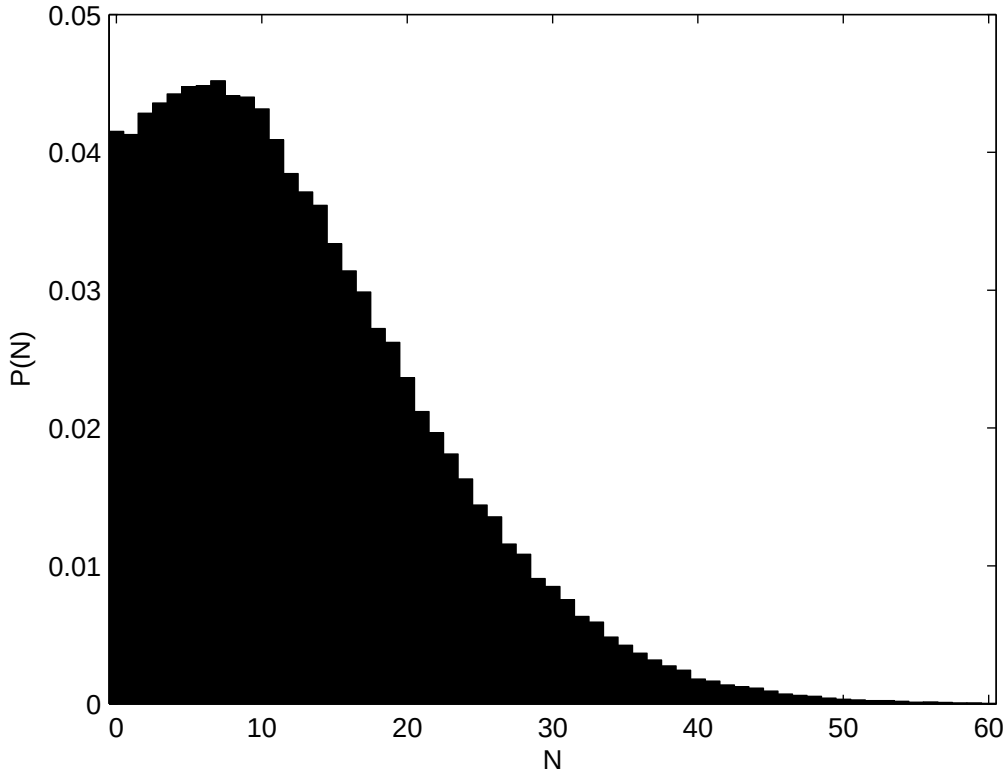

Figure 2: The probability distribution of observing N MSPs from the spherical bulge population based on a lognormal luminosity function fitted assuming only MSPs from the disk model can be observed.

bulge MSPs. This could reduce the likelihood for luminosity functions that tend to generate high luminosity MSPs with greater probability. Figure 1 shows the luminosity function parameter distribution which results when the contribution of resolved bulge MSPs is removed. Based on the fitted flux threshold, we found a mean of 12.8 resolved spherical bulge MSPs, and the probability of observing one or more was 0.959. The probability distribution is shown in figure 2. It is also suggested in ref. [27] that a further restriction can be placed on the luminosity function parameters by considering MSPs located in globular clusters. These were not taken into account here as it is unlikely they would have the same luminosity distribution as the disk population. It is concluded in ref. [27] that many MSPs located in the bulge should have already been observed if the luminosity distribution were the same for disk and bulge MSPs. We find that there is a significant probability that no bulge MSPs would have been resolved based on the fitted threshold and luminosity function parameters. Although six of the observed MSPs are inside the solid angle of the projected spherically symmetric bulge, the distances estimated using dispersion measures indeed indicate that none are actually located inside this bulge. With four times the current sensitivity to point sources it is likely that many bulge MSPs could be resolved. Double the current sensitivity could result in a few observations.

4. Conclusions

An MCMC algorithm was used to constrain parameters for a set of models of the Milky Way MSP population, with the luminosity distribution being of particular interest. This search over the parameter space was performed using the GCE data, the locations of observed MSPs in the sky, their fluxes, and their distances where parallax distance measurements were available.

To confirm that the models could plausibly explain the observations, the Markov chains of parameters produced by the MCMC simulation were then used to produce simulated data. The simulated distributions of resolved MSPs were a good fit to the observed data, as were the simulations of the GCE.

Although it seems unlikely that the disk and bulge MSPs would have the same luminosity function, our results show that the current data are not precise enough to reveal any differences between the two (if they exist). This is mainly because the bulge MSP population is relatively unconstrained by our analysis which is only sensitive to the luminosity of the entire population via the product $\bar{L}N_{\rm bulge}$ where $\bar{L}$ is the average luminosity. While the constraint that not too many bright, bulge MSPs be predicted does require that the luminosity function not be too skewed too much towards high luminosities, this turns out not to be a very tight constraint given the current point source sensitivity of observations towards the inner Galaxy.

It was claimed by ref. [27] that if the GCE were produced by MSPs, many of them would already have been resolved. Here, it has been shown that this is in fact not the case. The main cause of this disagreement is likely due to ref. [27] not including the possibility of resolved bulge MSPs when they evaluated their best fit luminosity function parameters.

Acknowledgments

We thank David Smith for providing the numerical values for figure 16 of ref. [30] and also for helpful correspondence. We gratefully acknowledge useful correspondence and conversation with Lilia Ferrario, Dan Hooper, Ivo Seitenzahl, Ashley Ruiter, Simone Scaringi, and Qiang Yuan.

References

[1] H. Ploeg, C. Gordon, R. Crocker and O. Macias, *Consistency between the luminosity function of resolved millisecond pulsars and the galactic center excess*, *J.~Cosm.~&~Astropart.~Phys.* **8** (Aug., 2017) 015, [1705.00806].

[2] L. Goodenough and D. Hooper, *Possible Evidence For Dark Matter Annihilation In The Inner Milky Way From The Fermi Gamma Ray Space Telescope*, *ArXiv e-prints (arXiv:0910.2998)* (Oct., 2009) , [0910.2998].

[3] D. Hooper and T. Linden, *On The Origin Of The Gamma Rays From The Galactic Center*, *Phys.~Rev.* **D84** (2011) 123005, [1110.0006].

[4] K. N. Abazajian and M. Kaplinghat, *Detection of a Gamma-Ray Source in the Galactic Center Consistent with Extended Emission from Dark Matter Annihilation and Concentrated Astrophysical Emission*, *Phys.~Rev.* **D86** (2012) 083511, [1207.6047].

[5] C. Gordon and O. Macias, *Dark Matter and Pulsar Model Constraints from Galactic Center Fermi-LAT Gamma Ray Observations*, *Phys.~Rev.* **D88** (2013) 083521, [1306.5725].

[6] O. Macias and C. Gordon, *Contribution of cosmic rays interacting with molecular clouds to the Galactic Center gamma-ray excess*, *Phys. Rev.* **D89** (2014) 063515, [1312.6671].

[7] K. N. Abazajian, N. Canac, S. Horiuchi and M. Kaplinghat, *Astrophysical and Dark Matter Interpretations of Extended Gamma-Ray Emission from the Galactic Center*, *Phys. Rev.* **D90** (2014) 023526, [1402.4090].

[8] T. Daylan, D. P. Finkbeiner, D. Hooper, T. Linden, S. K. N. Portillo, N. L. Rodd et al., *The characterization of the gamma-ray signal from the central Milky Way: A case for annihilating dark matter*, *Phys. Dark Univ.* **12** (2016) 1–23, [1402.6703].

[9] B. Zhou, Y.-F. Liang, X. Huang, X. Li, Y.-Z. Fan, L. Feng et al., *GeV excess in the Milky Way: The role of diffuse galactic gamma-ray emission templates*, *Phys. Rev.* **91** (June, 2015) 123010, [1406.6948].

[10] F. Calore, I. Cholis and C. Weniger, *Background model systematics for the Fermi GeV excess*, *J.~Cosm.~&~Astropart.~Phys.* **3** (Mar., 2015) 38, [1409.0042].

[11] FERMI-LAT collaboration, M. Ajello et al., *Fermi-LAT Observations of High-Energy γ-Ray Emission Toward the Galactic Center*, *Astrophys.~J.* **819** (2016) 44, [1511.02938].

[12] C. Karwin, S. Murgia, T. M. P. Tait, T. A. Porter and P. Tanedo, *Dark Matter Interpretation of the Fermi-LAT Observation Toward the Galactic Center*, *Phys. Rev.* **D95** (2017) 103005, [1612.05687].

[13] The Fermi-LAT Collaboration, *The Fermi Galactic Center GeV Excess and Implications for Dark Matter*, *ArXiv e-prints* (Apr., 2017) , [1704.03910].

[14] S. K. Lee, M. Lisanti, B. R. Safdi, T. R. Slatyer and W. Xue, *Evidence for Unresolved γ -Ray Point Sources in the Inner Galaxy*, *Phys.~Rev.~Lett.* **116** (Feb., 2016) 051103, [1506.05124].

[15] R. Bartels, S. Krishnamurthy and C. Weniger, *Strong Support for the Millisecond Pulsar Origin of the Galactic Center GeV Excess*, *Phys.~Rev.~Lett.* **116** (Feb., 2016) 051102, [1506.05104].

[16] FERMI-LAT collaboration, M. Ajello et al., *Characterizing the population of pulsars in the Galactic bulge with the Fermi Large Area Telescope*, *Submitted to: Astrophys. J.* (2017) , [1705.00009].

[17] S. Horiuchi, M. Kaplinghat and A. Kwa, *Investigating the Uniformity of the Excess Gamma rays towards the Galactic Center Region*, *JCAP* **1611** (2016) 053, [1604.01402].

[18] K. N. Abazajian, *The Consistency of Fermi-LAT Observations of the Galactic Center with a Millisecond Pulsar Population in the Central Stellar Cluster*, *J.~Cosm.~&~Astropart.~Phys.* **1103** (2011) 010, [1011.4275].

[19] Q. Yuan and B. Zhang, *Millisecond pulsar interpretation of the Galactic center gamma-ray excess*, *J.~High~Energy~Astrophys.* **3** (Sept., 2014) 1–8, [1404.2318].

[20] R. M. O'Leary, M. D. Kistler, M. Kerr and J. Dexter, *Young Pulsars and the Galactic Center GeV Gamma-ray Excess*, *ArXiv e-prints (arXiv:1504.02477)* (Apr., 2015) , [1504.02477].

[21] W. Wang, Z. J. Jiang and K. S. Cheng, *Contribution to diffuse gamma-rays in the Galactic Centre region from unresolved millisecond pulsars*, *Mon.~Not.~R.~Astron.~Soc.* **358** (Mar., 2005) 263–269, [astro-ph/0501245].

[22] T. D. Brandt and B. Kocsis, *Disrupted Globular Clusters Can Explain the Galactic Center Gamma Ray Excess*, *Astrophys. J.* **812** (2015) 15, [1507.05616].

[23] O. Y. Gnedin, J. P. Ostriker and S. Tremaine, *Co-evolution of Galactic Nuclei and Globular Cluster Systems*, *ApJ* **785** (Apr., 2014) 71, [1308.0021].

[24] F. Camilo and F. A. Rasio, *Pulsars in Globular Clusters*, in *Binary Radio Pulsars* (F. A. Rasio and I. H. Stairs, eds.), vol. 328 of *Astronomical Society of the Pacific Conference Series*, p. 147, July, 2005. astro-ph/0501226.

[25] FERMI-LAT collaboration, F. Acero, M. Ackermann, M. Ajello, A. Albert et al., *Fermi Large Area Telescope Third Source Catalog*, *Astrophys. J. Supp.* **218** (June, 2015) 23, [1501.02003].

[26] R. N. Manchester, G. B. Hobbs, A. Teoh and M. Hobbs, *The Australia Telescope National Facility Pulsar Catalogue*, *Astron.~J.* **129** (Apr., 2005) 1993–2006, [astro-ph/0412641].

[27] D. Hooper and G. Mohlabeng, *The gamma-ray luminosity function of millisecond pulsars and implications for the GeV excess*, *Journal of Cosmology and Astroparticle Physics* **2016** (2016) 049.

[28] C.-A. Faucher-Giguère and A. Loeb, *The Pulsar Contribution to the Gamma-Ray Background*, *JCAP* **1** (2010) 005, [0904.3102].

[29] P. G. Mezger, W. J. Duschl and R. Zylka, *The galactic center: a laboratory for agn?*, *The Astronomy and Astrophysics Review* **7** (Dec, 1996) 289–388.

[30] FERMI-LAT collaboration, A. Abdo et al., *The Second Fermi Large Area Telescope Catalog of Gamma-ray Pulsars*, *Astrophys. J. Supp.* **208** (2013) 17, [1305.4385].

[31] H. Haario, E. Saksman and J. Tamminen, *An adaptive Metropolis algorithm*, *Bernoulli* **7** (2001) 223–242.

[32] W. Cash, *Parameter estimation in astronomy through application of the likelihood ratio*, *ApJ* **228** (Mar., 1979) 939–947.

[33] S. A. Story, P. L. Gonthier and A. K. Harding, *Population synthesis of radio and gamma-ray millisecond pulsars from the Galactic disk*, *Astrophys. J.* **671** (2007) 713–726, [0706.3041].

[34] T. Grégoire and J. Knödlseder, *Constraining the Galactic millisecond pulsar population using Fermi Large Area Telescope*, *Astron. Astrophys.* **554** (2013) A62, [1305.1584].

[35] D. R. Lorimer, *The Galactic Millisecond Pulsar Population*, in *Neutron Stars and Pulsars: Challenges and Opportunities after 80 years* (J. van Leeuwen, ed.), vol. 291 of *IAU Symposium*, pp. 237–242, Mar., 2013. 1210.2746. DOI.

[36] V. Korolev and I. Shevtsova, *An improvement of the berry-esseen inequality with applications to poisson and mixed poisson random sums*, *Scandinavian Actuarial Journal* **2012** (2012) 81–105, [http://dx.doi.org/10.1080/03461238.2010.485370].

[37] O. Macias, C. Gordon, R. M. Crocker, B. Coleman, D. Paterson, S. Horiuchi et al., *Discovery of Gamma-Ray Emission from the X-shaped Bulge of the Milky Way*, 1611.06644.

[38] A. Gelman, J. Carlin, H. Stern, D. Dunson, A. Vehtari and D. Rubin, *Bayesian Data Analysis*. CRC Press, 3 ed.

[39] G. Mohlabeng. Personal communication, Nov., 2016.